

AD-A142 016

A PROBABILISTIC ONE-DIMENSIONAL GROUND-SHOCK CODE FOR
LAYERED NONLINEAR H..(U) ARMY ENGINEER WATERWAYS
EXPERIMENT STATION VICKSBURG MS STRUC..

1/1

UNCLASSIFIED

B ROHANI ET AL. APR 84 WES/MP/SL-84-6

F/G 19/4

NL

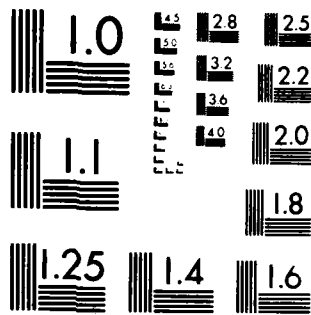
END

DATE

FILED

7-84

DTIC



MICROCOPY RESOLUTION TEST CHART
NATIONAL BUREAU OF STANDARDS 1963-A



US Army Corps
of Engineers

AD-A142 016

MISCELLANEOUS PAPER SL-84-6

12

A PROBABILISTIC ONE-DIMENSIONAL GROUND-SHOCK CODE FOR LAYERED NONLINEAR HYSTERETIC MATERIALS

by

Behzad Rohani and James D. Cargile

Structures Laboratory

U. S. Army Engineer Waterways Experiment Station
P. O. Box 631, Vicksburg, Miss. 39180



April 1984

Final Report

Approved For Public Release: Distribution Unlimited

DTIC
ELECTE
JUN 12 1984
B

DTIC FILE COPY



Prepared for Office, Chief of Engineers, U. S. Army
Washington, D. C. 20314

Under Project 4A162719AT40
Task AO, Work Unit 024

84 06 11 008

Destroy this report when no longer needed. Do not
return it to the originator.

The findings in this report are not to be construed as an
official Department of the Army position unless so
designated by other authorized documents.

The contents of this report are not to be used for
advertising, publication, or promotional purposes.
Citation of trade names does not constitute an
official endorsement or approval of the use of such
commercial products.

Unclassified

SECURITY CLASSIFICATION OF THIS PAGE (When Data Entered)

REPORT DOCUMENTATION PAGE		READ INSTRUCTIONS BEFORE COMPLETING FORM
1. REPORT NUMBER Miscellaneous Paper SL-84-6	2. GOVT ACCESSION NO. A1462016	3. RECIPIENT'S CATALOG NUMBER
4. TITLE (and Subtitle) A PROBABILISTIC ONE-DIMENSIONAL GROUND-SHOCK CODE FOR LAYERED NONLINEAR HYSTERETIC MATERIALS		5. TYPE OF REPORT & PERIOD COVERED Final Report
7. AUTHOR(s) Behzad Rohani James D. Cargile		6. PERFORMING ORG. REPORT NUMBER
9. PERFORMING ORGANIZATION NAME AND ADDRESS U. S. Army Engineer Waterways Experiment Station Structures Laboratory P. O. Box 631, Vicksburg, Miss. 39180		8. CONTRACT OR GRANT NUMBER(s)
11. CONTROLLING OFFICE NAME AND ADDRESS Office, Chief of Engineers, U. S. Army Washington, D. C. 20314		10. PROGRAM ELEMENT, PROJECT, TASK AREA & WORK UNIT NUMBERS Project 4A162719AT40, Task A0, Work Unit 024
14. MONITORING AGENCY NAME & ADDRESS (if different from Controlling Office)		12. REPORT DATE April 1984
		13. NUMBER OF PAGES 37
		15. SECURITY CLASS. (of this report) Unclassified
		15a. DECLASSIFICATION/DOWNGRADING SCHEDULE
16. DISTRIBUTION STATEMENT (of this Report) Approved for public release; distribution unlimited.		
17. DISTRIBUTION STATEMENT (of the abstract entered in Block 20, if different from Report)		
18. SUPPLEMENTARY NOTES Available from National Technical Information Service, 5285 Port Royal Road, Springfield, VA 22161.		
19. KEY WORDS (Continue on reverse side if necessary and identify by block number) Airblast-induced ground shock Probabilistic analysis Numerical analysis Soil property uncertainties One-dimensional plane wave propagation		
20. ABSTRACT (Continue on reverse side if necessary and identify by block number) The ground-shock calculation codes currently used to predict states of stress and ground motion induced in natural earth masses by explosive detonations are deterministic tools; that is, their input parameters (site layering, material density, stress-strain and strength properties, surface airblast prescriptions, etc.) are specified as single-valued quantities. In reality, however, both the properties of earth materials and the characteristics of explosive pulses are random variables. Consequently, the resultant (Continued)		

DD FORM 1 JAN 73 1473 EDITION OF 1 NOV 65 IS OBSOLETE

Unclassified

SECURITY CLASSIFICATION OF THIS PAGE (When Data Entered)

Unclassified

SECURITY CLASSIFICATION OF THIS PAGE(When Data Entered)

20. ABSTRACT (Continued)

states of stress and ground motion in a given earth mass are also random variables and, therefore, ground shock problems should be analyzed probabilistically.

This report describes the conversion of the WES ONED code (a deterministic one-dimensional plane wave propagation code which treats the response of layered nonlinear hysteretic media to airslap loadings) into a probabilistic code using the partial derivative method (also referred to as the Taylor-series approximation method). This approach requires the execution of $2n+1$ deterministic calculations to establish the effects of n independent (random) input variables encompassed in a given problem on the output variables (time histories of stress, particle velocity, and displacement). The probabilistic code then calculates the expected values of these time histories and their variances. All partial derivatives are evaluated numerically using finite-difference approximations. The merits of this probabilistic solution technique are demonstrated for an actual field explosive test and the code is evaluated against a closed-form probabilistic solution.

Unclassified

SECURITY CLASSIFICATION OF THIS PAGE(When Data Entered)

PREFACE

The work reported herein was conducted at the U. S. Army Engineer Waterways Experiment Station (WES) under the sponsorship of the Office, Chief of Engineers, Department of the Army, as part of Project 4A162719AT40, Task A0, Work Unit 024, "Ground-Shock Prediction Techniques for Earth and Earth-Structure Systems."

This study was conducted by Dr. Behzad Rohani and Mr. James D. Cargile under the direction of Dr. J. G. Jackson, Jr., Chief, Geomechanics Division (GD), Structures Laboratory (SL). Mr. Bryant Mather was Chief, SL. The authors are grateful to Dr. J. S. Zelasko (GD) for suggesting the problem of Appendix A and constructing its analytic solution.

COL Tilford C. Creel, CE, was the Commander and Director of WES during this investigation. Mr. F. R. Brown was Technical Director.



Accession For	
NTIS GRA&I	<input checked="checked" type="checkbox"/>
DTIC TAB	<input type="checkbox"/>
Unannounced	<input type="checkbox"/>
Justification	
By	
Distribution/	
Availability Codes	
Dist	Avail and/or Special
A-1	

CONTENTS

	<u>Page</u>
PREFACE	1
CONVERSION FACTORS, NON-SI TO SI (METRIC) UNITS OF MEASUREMENT	3
PART I: INTRODUCTION	4
PART II: BRIEF DESCRIPTION OF THE DETERMINISTIC ONED CODE	6
PART III: PROBABILISTIC ANALYSIS	8
PART IV: NUMERICAL EXAMPLE	12
PART V: SUMMARY	27
REFERENCES	28
TABLE 1	
APPENDIX A: COMPARISON OF CODE CALCULATION WITH ANALYTICAL SOLUTION	A1
APPENDIX B: NOTATION	B1

CONVERSION FACTORS, NON-SI TO SI (METRIC)
UNITS OF MEASUREMENT

Non-SI units of measurement used in this report can be converted to SI (metric) units as follows:

<u>Multiply</u>	<u>By</u>	<u>To Obtain</u>
feet	0.3048	metres
inches	2.54	centimetres
inches per second	0.0254	metres per second
pounds (mass) per cubic foot	1.601846E+01	kilograms per cubic metre
pounds (force) per square inch	6.894757	kilopascals

A PROBABILISTIC ONE-DIMENSIONAL GROUND-SHOCK CODE
FOR LAYERED NONLINEAR HYSTERETIC MATERIALS

PART I: INTRODUCTION

1. The ground-shock calculation techniques currently used to predict the states of stress and ground motions induced in earth masses by explosive detonations are deterministic tools--that is, their input parameters (media stress-strain and strength properties, density, location of layer interfaces, surface airblast loadings, etc.) are specified as deterministic quantities or functions. In actuality, however, both the properties of earth materials and the characteristics of airblast pulses are random variables. Consequently, the randomness of these input variables dictates that resulting stresses and ground motions are also random variables; therefore, ground-shock problems should be analyzed probabilistically.

2. In general, ground shock from explosive bursts is a two-dimensional (2D) problem. However, when superseismic conditions prevail, as often happens in airslap problems, one-dimensional (1D) plane-wave analyses are quite adequate for predicting free-field responses. It is both useful and appropriate, therefore, to commence an examination of 1D probabilistic ground shock prior to investigating the more cumbersome 2D problem. A deterministic 1D wave-propagation code (ONED) developed and used extensively at the U. S. Army Engineer Waterways Experiment Station (WES 1971) was the tool selected for this task. ONED is a finite-difference code that treats arbitrary airslap prescriptions and layered nonlinear hysteretic materials.

3. This report describes the conversion of the ONED code into a probabilistic code using the method of partial derivatives (Benjamin and Cornell 1970). The method of partial derivatives (also referred to as the Taylor-series approximation method) greatly alleviates the burden of conducting brute force Monte Carlo analyses for probabilistic wave propagation problems. Furthermore, the partial-derivative method has the advantage that it can be used to quantitatively rank the relative effects of input variabilities (uncertainties) on the dispersion of the output quantities.

4. In Part II, the deterministic ONED code is briefly described, and in Part III the probabilistic solution is formulated. The merits of this

probabilistic solution technique are demonstrated for an actual field explosive test in Part IV. The work is summarized in Part V. The probabilistic code is evaluated against a closed-form solution in Appendix A.

PART II: BRIEF DESCRIPTION OF THE DETERMINISTIC ONED CODE

5. The ONED code is described in great detail by Radhakrishnan and Rohani (1971). Only the briefest description of the code (necessary for undertaking the subsequent development of the probabilistic solution) is presented in this part. ONED is based on a discrete model of continuum, consisting of a series of lumped masses interconnected by springs and dash-pots. An arbitrary dynamic pressure (with a finite rise time) is applied at the free (ground) surface. The equations of motion governing the dynamics of the mass-spring system are integrated in a step-by-step manner using Newmark's β -integration scheme. The code uses piecewise linear stress-strain relations for both loading and unloading in order to closely approximate the nonlinear hysteretic stress-strain curves of real earth materials. Provisions are made in the computer code to input realistic tension cutoffs (material tensile strengths) for each individual layer. The user must specify either a rigid or an infinite bottom boundary condition. Code output consists of time histories of stress σ , particle velocity \dot{U} , and particle displacement U at selected depths within the medium.

6. The basic code input for a generic layer I is shown in Figure 1 and consists of four blocks of information:

SS(I) = stress-strain relationship of the material

T(I) = tensile strength of the material

$\gamma(I)$ = density of the material

Z(I) = depth to the bottom of the layer from the surface

Therefore, including the surface pressure-time history $P(t)$, $4m+1$ input blocks are required for a problem consisting of m layers.

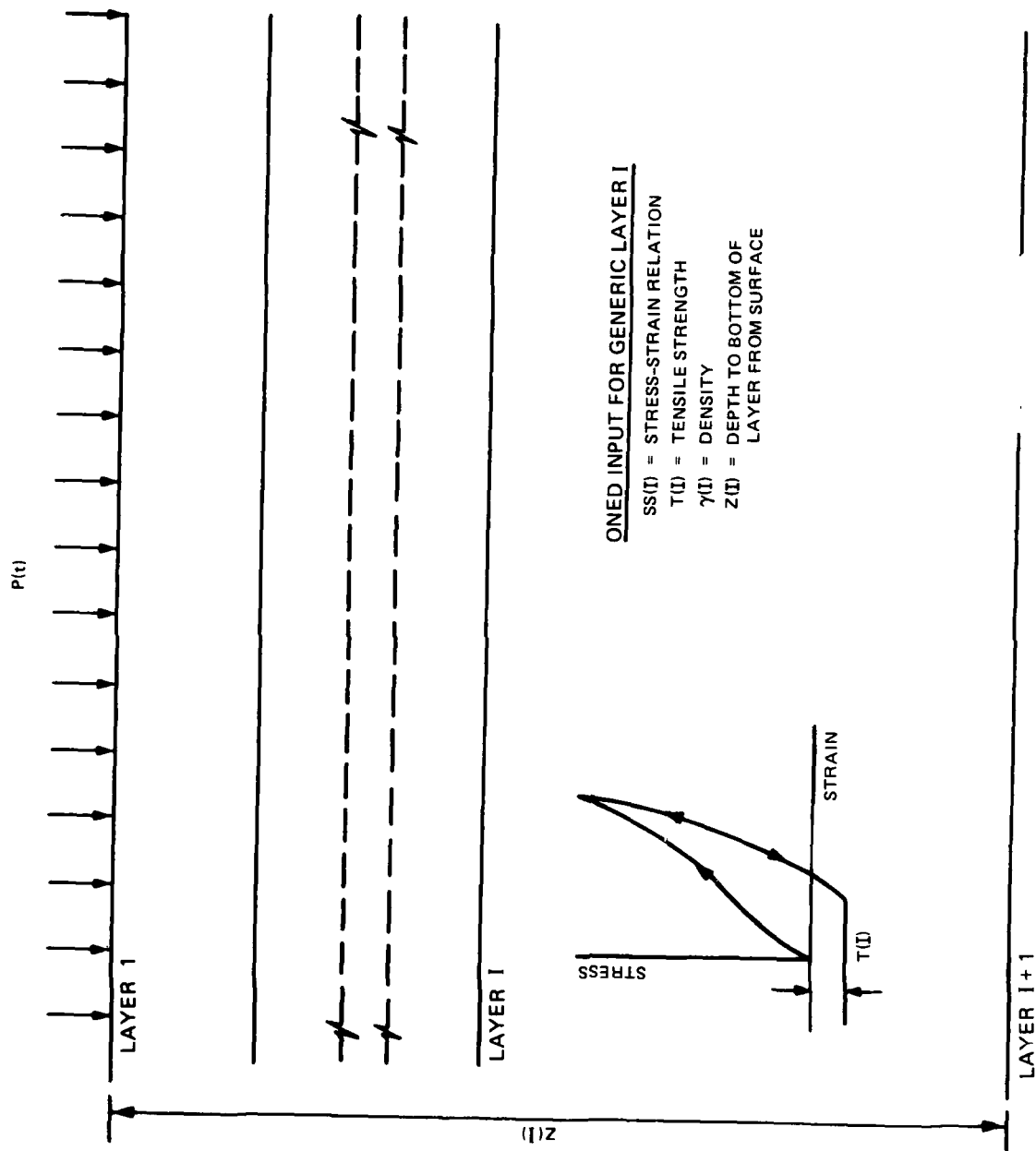


Figure 1. Description of ONED input for a generic layer I

PART III: PROBABILISTIC ANALYSIS

7. The purpose of a probabilistic analysis is to obtain a quantitative understanding of how the variabilities or uncertainties in (independent) input parameters for a particular problem affect the dispersion of the dependent output variables. An extremely useful procedure for implementing such an analysis is to apply the method of partial derivatives (Benjamin and Cornell 1970, Haugen 1968) to a deterministic scheme for solving the problem. The method gives approximations for the moments of the dependent variables in terms of functions of the moments of the independent variables. For example, if a random variable Y is functionally related to the random variables X_i

$$Y = Y(X_1, X_2, \dots, X_n) \quad (1)$$

and if the X_i are uncorrelated, then according to the partial derivative method the approximations for the expected value of Y , $E[Y]$, and the variance of Y , $\text{Var}[Y]$, are

$$E[Y] \approx Y(\mu_1, \mu_2, \dots, \mu_n) + \frac{1}{2} \sum_{i=1}^n \frac{\partial^2 Y}{\partial X_i^2} \bigg|_{(\mu_1, \mu_2, \dots, \mu_n)} \text{Var}[X_i] \quad (2)$$

$$\text{Var}[Y] \approx \sum_{i=1}^n \left(\frac{\partial Y}{\partial X_i} \bigg|_{(\mu_1, \mu_2, \dots, \mu_n)} \right)^2 \text{Var}[X_i] \quad (3)$$

where $(\mu_1, \mu_2, \dots, \mu_n)$ denotes the respective means of the random variables (X_1, X_2, \dots, X_n) . The first term on the right-hand side of Equation 2 corresponds to the mean value of Y , i.e., the value of Y obtained using the mean values of all of the random variables. The second term represents the contributions to the expected value of Y due to uncertainties in the X_i . This second term is negligible if $\text{Var}[X_i]$ and the nonlinearity in the function Y itself are not large.

8. As pointed out by Benjamin and Cornell (1970), Equation 3 "may be interpreted as meaning that each of the n random variables X_i contributes to the dispersion of Y in a manner proportional to its own variance

$\text{Var}[X_i]$ and proportional to a factor $\left(\frac{\partial Y}{\partial X_i} \bigg|_{(\mu_1, \mu_2, \dots, \mu_n)} \right)^2$, which is

related to the sensitivity of changes in Y to changes in X_i ." Thus, this equation can be used to conduct sensitivity analyses to quantify and rank the relative effects of the individual input variabilities or uncertainties on the dispersion of the output quantities.

9. The partial derivatives in Equations 2 and 3 can be evaluated analytically if an explicit expression is available for the dependent variable Y . However, as pointed out by Mlakar (1978), in many cases, even when such an explicit relation exists, it is often more convenient to evaluate the partial derivatives numerically using finite-difference approximations. Following the method proposed by Mlakar (1978), the partial derivatives may be expressed numerically as

$$\frac{\partial Y}{\partial X_i} = \frac{Y(\mu_1, \dots, \mu_i + kS_i, \dots, \mu_n) - Y(\mu_1, \dots, \mu_i - kS_i, \dots, \mu_n)}{2kS_i} \quad (4)$$

$$\frac{\partial^2 Y}{\partial X_i^2} = \frac{Y(\mu_1, \dots, \mu_i - kS_i, \dots, \mu_n) - 2Y(\mu_1, \dots, \mu_i, \dots, \mu_n) + Y(\mu_1, \dots, \mu_i + kS_i, \dots, \mu_n)}{(kS_i)^2} \quad (5)$$

$$i = 1, 2, \dots, n$$

The first partial derivative (Equation 4) is calculated from the functional value of Y at k standard deviation kS_i above and below the mean value of

X_i (i.e., μ_i) where k^* is a constant and S_i is the standard deviation of X_i . Similarly, the second partial derivative (Equation 5) is calculated from the mean value of Y and the functional values of Y at kS_i above and below μ_i . Therefore, for a problem containing n random variables, the application of Equations 2 through 5 requires $2n+1$ "point estimates" of the function Y .

10. The ONED code is used to calculate the time histories of the dependent variables σ , \dot{U} , and U (at selected depths) for the requisite combinations of the independent input variables $P(t)$, $SS(I)$, $T(I)$, $\gamma(I)$, and $Z(I)$ shown in Table 1, where $I = 1, 2, \dots, m$ and m = number of layers in a problem. Note that for a problem consisting of m layers, where all input parameters are treated as random variables, a maximum of $2(4m+1)+1$ ONED calculations are required for subsequent probabilistic analysis. In practice, however, not all of these variables have to be treated probabilistically. For example, one may only be interested in the relative effects of uncertainties in the surface airblast loading versus uncertainties in the soil stress-strain properties in the topmost stratum. Therefore, the required number of ONED calculations can often be greatly reduced. The results of the ONED calculations are then used in Equations 2 through 5 to calculate the expected value and variance of each of the dependent variables. A computer program, referred to as PONEED, has been developed for the express purpose of numerically evaluating Equations 2 through 5 using the output from the ONED code. Within this program, computations are made at successive times at selected depths so that the time histories of the expected value and the

* The term kS_i in Equations 4 and 5 may be viewed as a finite difference mesh spacing.¹ The value of k is heuristically taken to be 1.0 by Mlakar (1978). However, if either the standard deviations S_i or the nonlinearity in the function Y are large, smaller values of k should be tried until the results are no longer affected by further reductions in k . In a recent probabilistic analysis of plane 1D wave propagation in homogeneous bilinear hysteretic material, k was parametrically varied from 1.0 to 0.1 in order to determine the sensitivity of the final results to variations in k (Rohani, 1982). This analysis indicated that reducing k by an order of magnitude changed the results by only 6 percent (on the average) and at most by 12 percent. Moreover, the bulk of these changes occurred in going from $k = 1.0$ to $k = 0.5$, because reducing the value of k from 0.5 to 0.1 only produced changes of 1 percent (on the average) and 3 percent (at most).

variance of the dependent variables σ , \dot{U} , and U can be constructed. To process the results of the ONED calculations, PONED first calculates an expected value for the arrival time of the wave at any selected depth (using the arrival time data from the individual ONED runs). PONED then translates (shifts) all the waveforms to this common arrival time for processing. PONED also computes and prints out explicit contributions of each of the input (independent) random variables to the overall dispersion of the various output quantities (dependent variables).

PART IV: NUMERICAL EXAMPLE

11. In this section we demonstrate the previously described methodology for conducting probabilistic wave propagation analysis by presenting an example problem. The example problem involves an actual field explosive experiment consisting of a homogeneous half-space of soil subjected to a decaying surface pressure-time history. The stress-strain properties of the soil and applied surface pressure are treated as random variables in this problem. Therefore, the probabilistic analysis of this problem would require five deterministic calculations using the ONED code. The input parameters for the problem are shown in Figures 2 through 4. Figure 2 portrays the surface pressure-time relation out to a real time of 30 msec, while Figure 3 shows the first 8 msec of these pulses on an expanded scale. These figures depict the mean μ and $\mu \pm kS$ time histories of the surface airblast pulse (corresponding to $k=1$) which were obtained from statistical analysis of nine blast pressure measurements (Jackson 1982). Figure 4 shows the mean μ and $\mu \pm S$ relations for the stress-strain properties of the soil. In Figure 4, the unloading slopes of all three stress-strain curves are equal. Therefore, the uncertainty in the soil properties is evaluated only for the loading portion of the stress-strain curve. The tensile strength of the material is presumed to be zero and deterministic. Moreover, since the uncertainty in the soil density is small, it too is assumed to be deterministic and equal to 116.0 lb/ft³.*

12. The five deterministic ONED calculations were conducted using the input parameters shown in Figures 2 and 4. In accordance with Table 1, the five calculations were conducted using the following combinations of random input parameters:

ONED Calculation	ONED Input	
	Surface Pressure-Time Relation	Stress-Strain Relation
1	μ	μ
2	μ	$\mu+S$
3	μ	$\mu-S$
4	$\mu+S$	μ
5	$\mu-S$	μ

* A table of factors for converting non-SI (metric) units of measurement is presented on page 3.

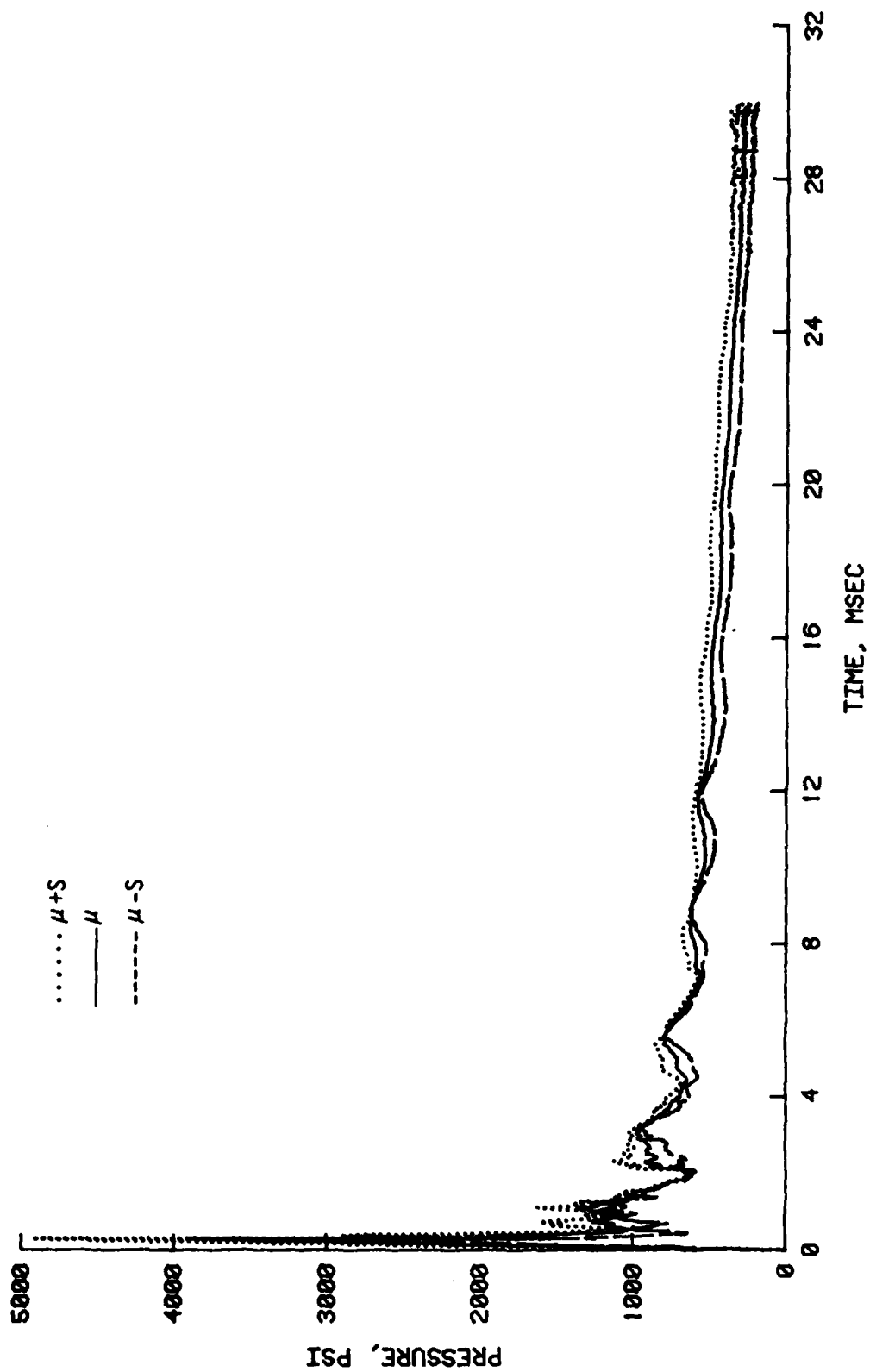


Figure 2. Surface pressure-time relations

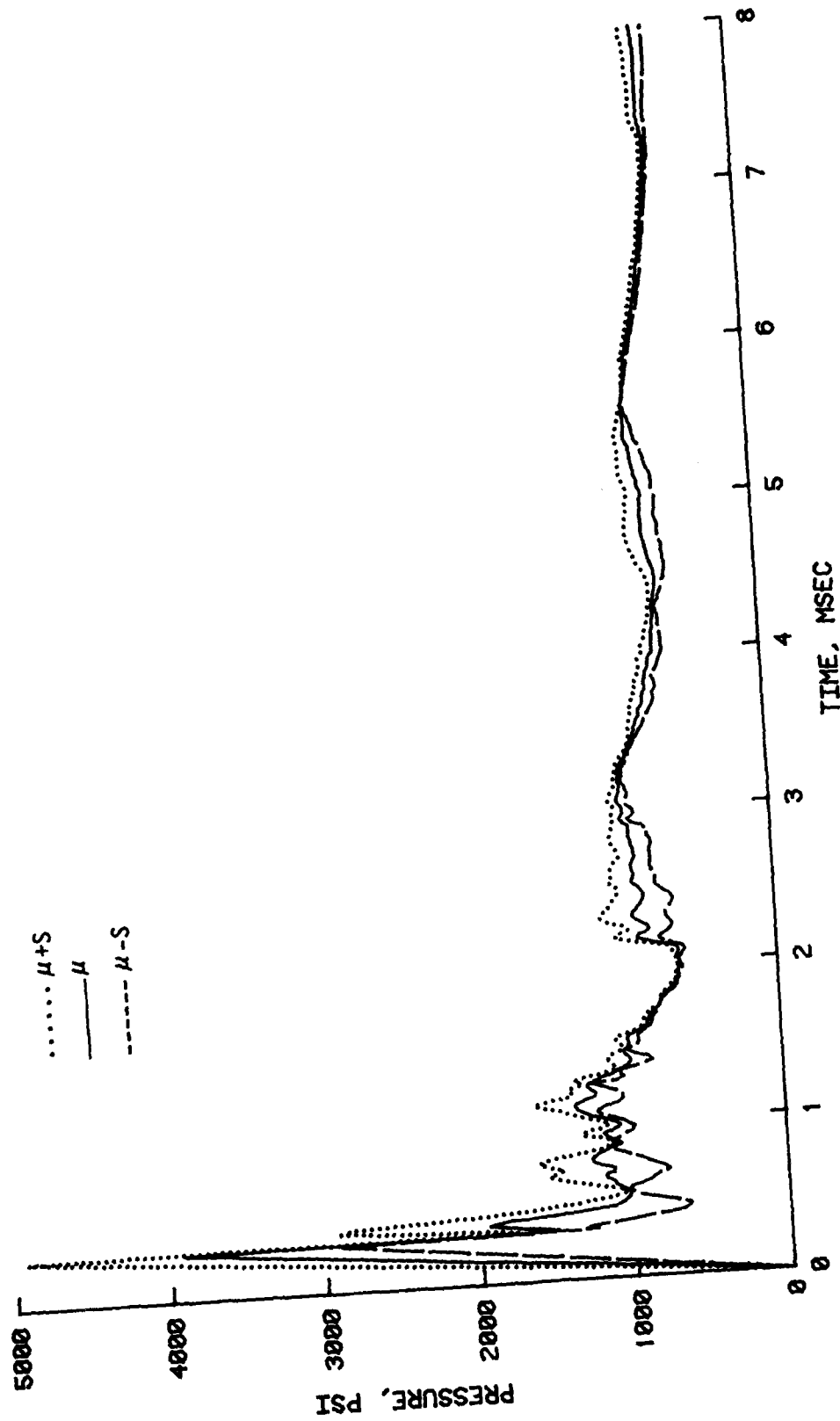


Figure 3. The first 8 msec of surface pressure-time relations

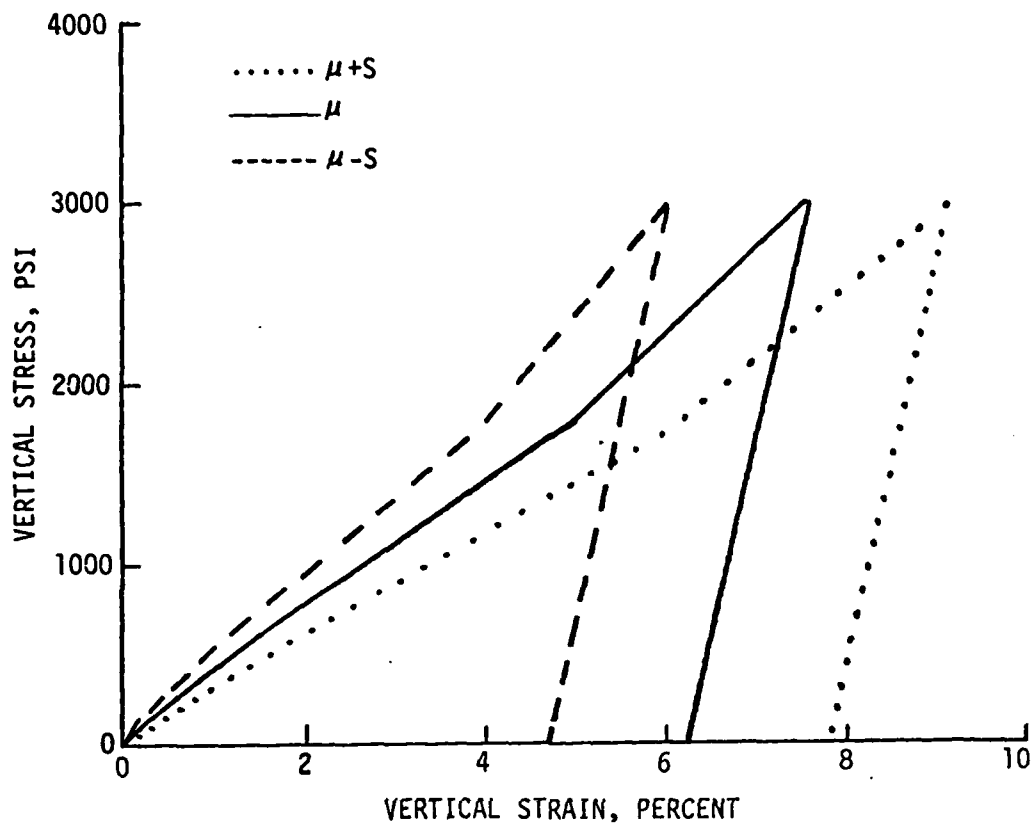


Figure 4. Stress-strain relations

The results of these calculations were processed with PONE in order to obtain the time histories of the expected values and variances of σ , \dot{U} , and U at selected depths. Probabilistic results are presented in Figures 5 through 10 for depths of 10, 15, and 20 ft. Figures 5, 7, and 9 show the expected values of stress $E[\sigma]$, particle velocity $E[\dot{U}]$, and particle displacement $E[U]$, respectively. The coefficients of variation of stress $V[\sigma]$, particle velocity $V[\dot{U}]$, and particle displacement $V[U]$ are shown in Figures 6, 8, and 10, respectively. As mentioned before, the arrival times for these plots at any depth correspond to the expected value of the arrival time at that depth.

13. From Figures 5 through 10, several interesting observations can be made regarding the wave propagation conditions for this problem. Consistent

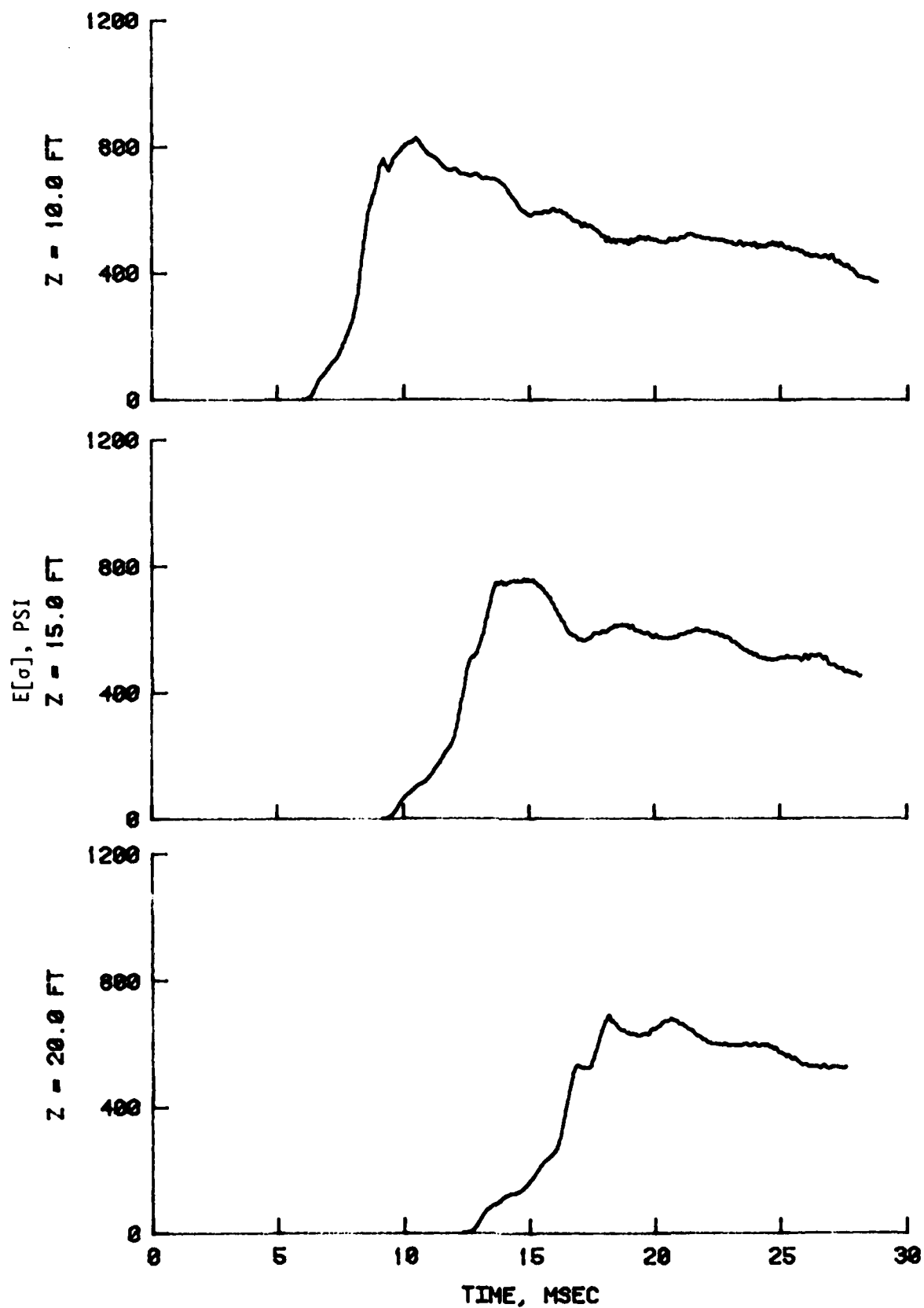


Figure 5. Time history of $E[\sigma]$ at selected depths

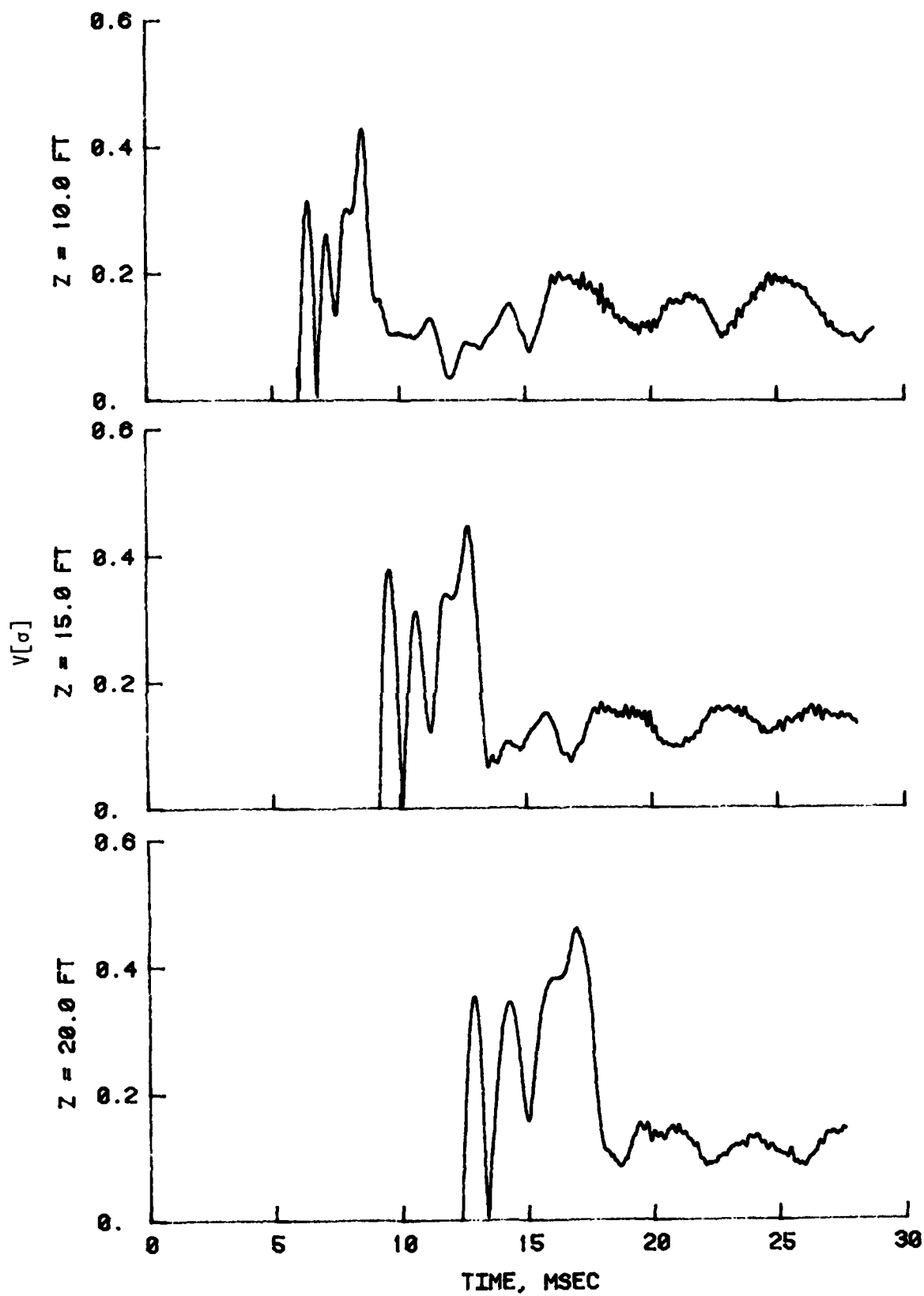


Figure 6. Time history of $V[\sigma]$ at selected depths

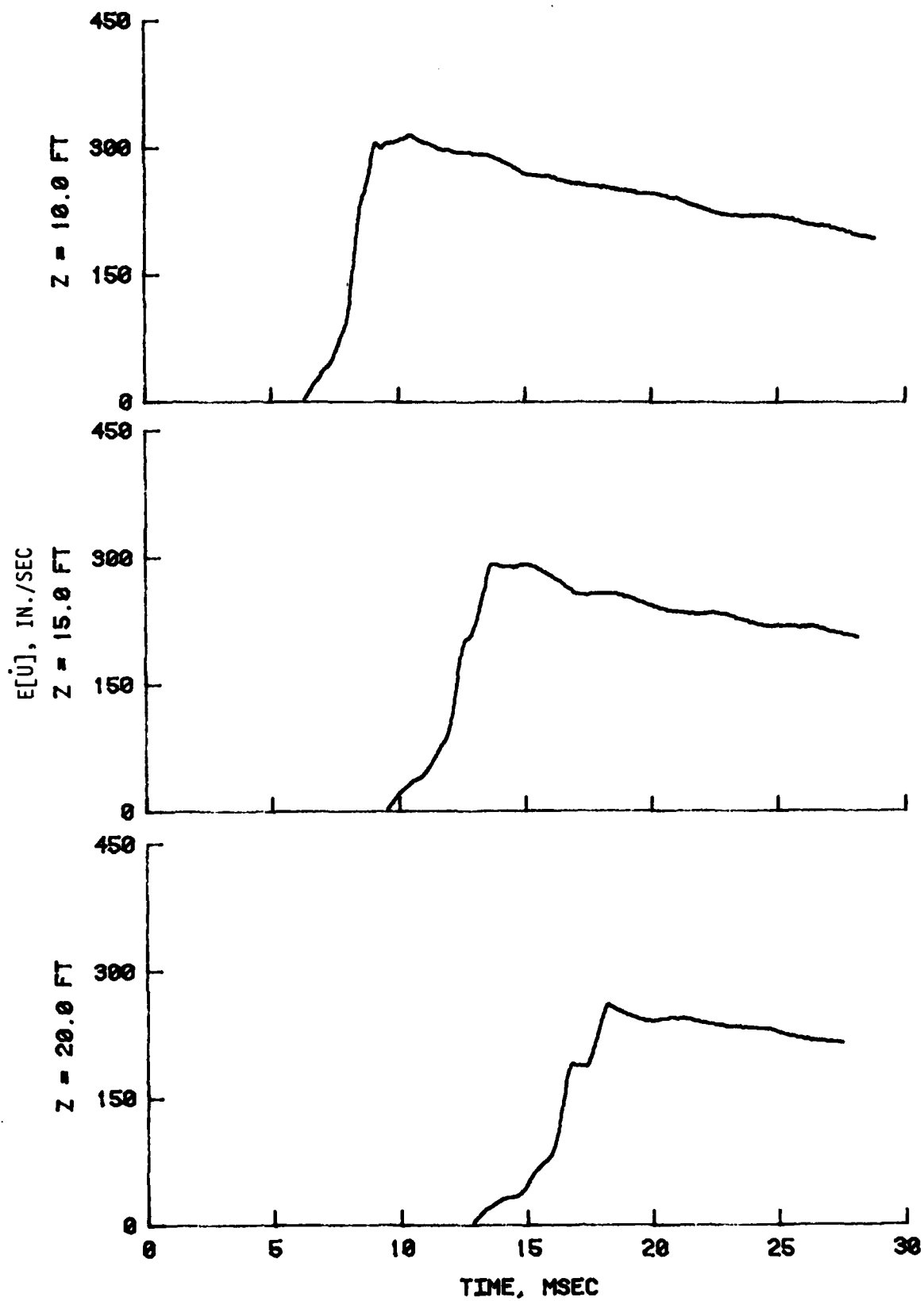


Figure 7. Time history of $E[\dot{U}]$ at selected depths

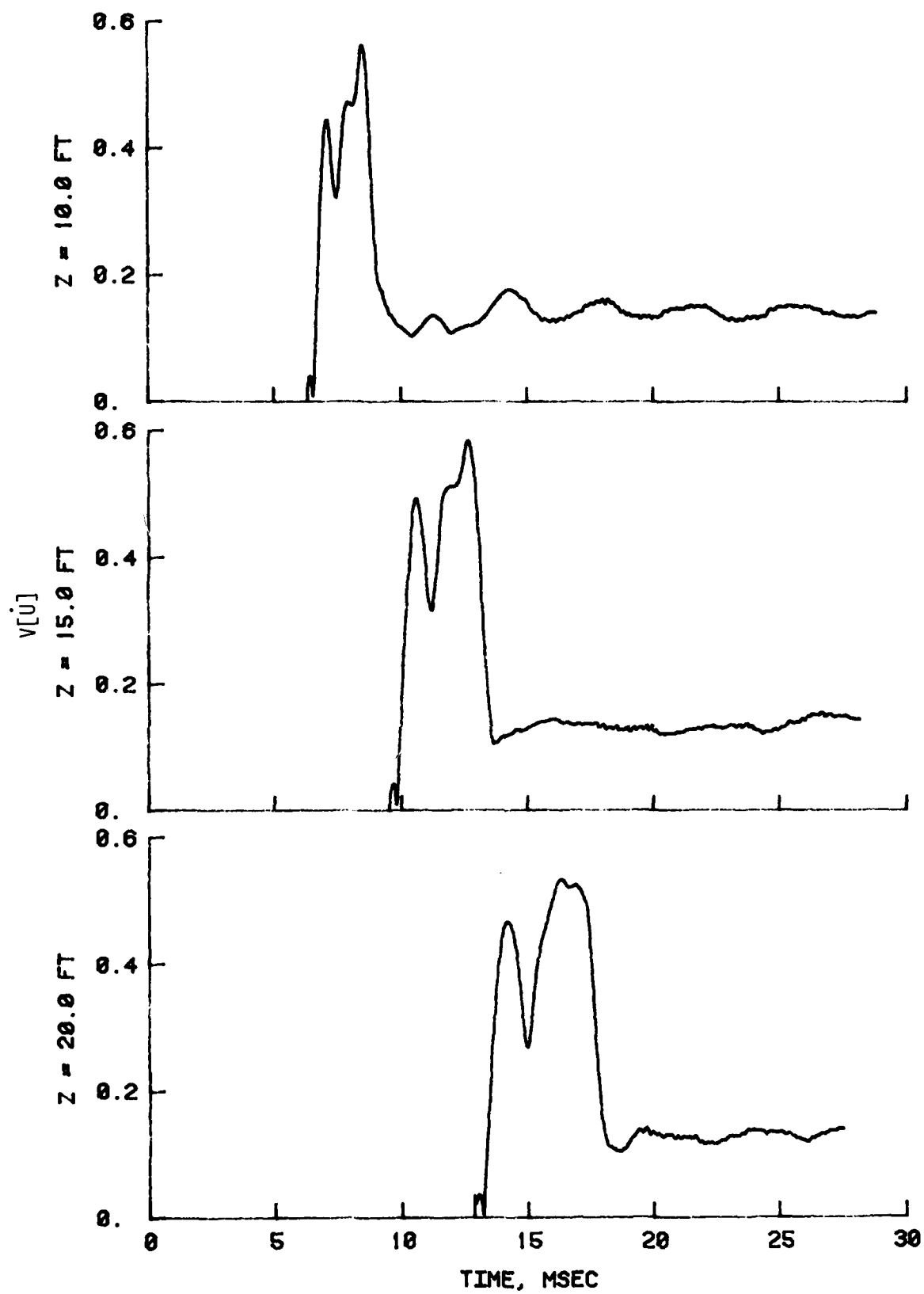


Figure 8. Time history of $V[\dot{U}]$ at selected depths

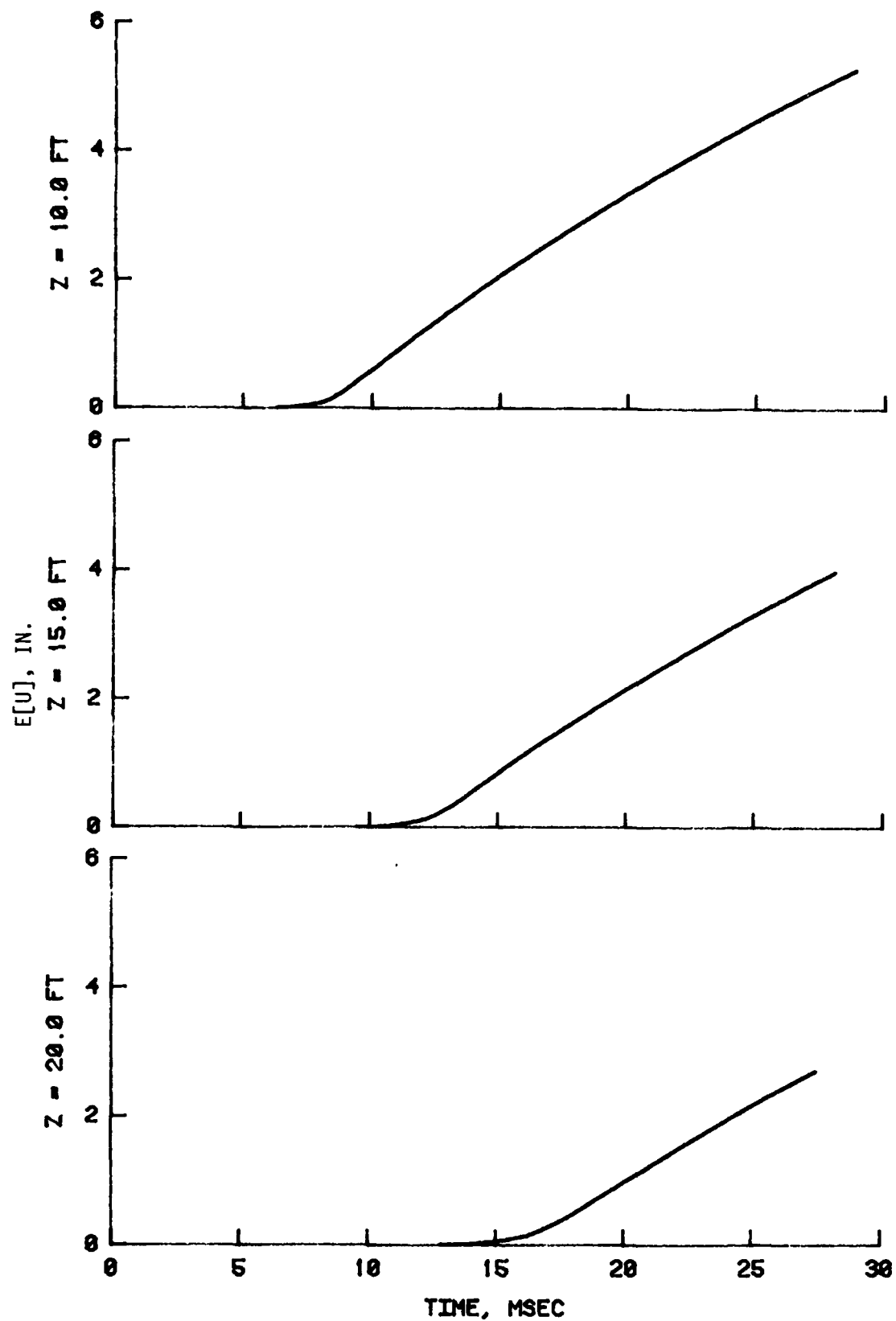


Figure 9. Time history of $E[U]$ at selected depths

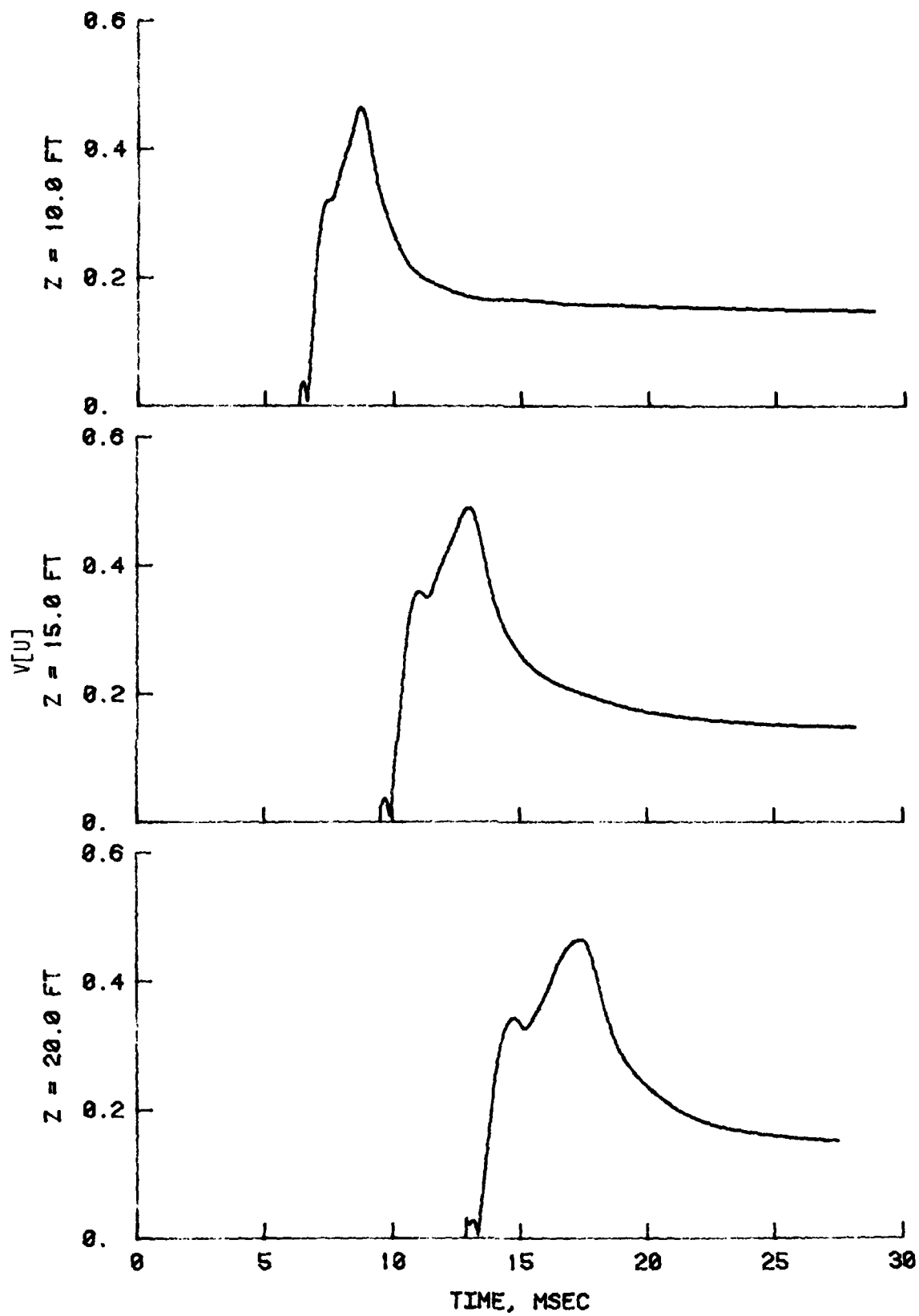


Figure 10. Time history of $V[U]$ at selected depths

with the input surface pressure-time histories, the expected values of stress (Figure 5) and particle velocity (Figure 7) initially increase with increasing time and then decay after reaching their peak values. Peak values, of course, attenuate with depth. The rise times of the waveforms, however, increase with increasing depth due to the slight "softening" or dispersive characteristics of the low-level stress-strain relations shown in Figure 4.

14. Turning now to Figures 6 and 8, it is observed that during the rise portion of the curves there are sudden changes in the values of the coefficients of variation, particularly in the case of stress (Figure 6). This type of behavior is real and is due to differences and/or similarities in the rise portions of the deterministic waveforms associated with each random variable. After reaching peak values, the coefficients of variation drop sharply and then oscillate around a constant value with increasing time. Therefore, the largest uncertainties are associated with the rise portion of the stress and particle velocity waveforms.

15. Two types of oscillations are recognized in Figures 6 and 8; low frequency and high frequency. The low-frequency oscillations are real and are due to the oscillatory nature of the input surface pressure-time relation (Figure 2). The high-frequency oscillations, however, are due to the numerical algorithm of the ONED code which introduces spurious oscillations in the code output (there are provisions in the ONED code to input viscous damping factors to substantially reduce such oscillations). Therefore, the uncertainties introduced in the probabilistic analysis due to this type of oscillation are not physical and are due to the solution technique itself. The magnitude of such uncertainties depends on many factors such as integration time step, grid size, and stress-strain properties of the material. To minimize these types of uncertainties, attempts should be made to reduce the spurious oscillations in the ONED code output by using either artificial viscosity or digital filtering.

16. The coefficient of variation of particle displacement (Figure 10) also drops after reaching peak value and eventually becomes constant. The expected value of particle displacement (Figure 9), of course, increases with increasing time.

17. Figures 11 through 13 demonstrate how the probabilistic method can be used to quantify and rank the relative effects of input uncertainties on

the dispersion of output quantities. These figures show, as a percentage, the contribution of each input uncertainty to the overall output uncertainty. In the case of stress (Figure 11) and particle velocity (Figure 12), the uncertainties during the rise portions of the waveforms are due entirely to uncertainty in soil compressibility (stress-strain relation). With increasing time, however, the contribution due to soil compressibility diminishes while the contribution due to airblast pressure steadily increases. This trend is due to the fact that the unloading portion of the soil stress-strain relations in Figure 4 was a constant and not a random variable. The contribution of input uncertainties to output uncertainty for particle displacement is shown in Figure 13. Again, during the early times (a time window corresponding to the rise portion of the particle velocity waveform), the uncertainty in output is due entirely to soil compressibility. The influence of soil compressibility gradually decreases with increasing time while the contribution due to airblast impulse gradually increases.

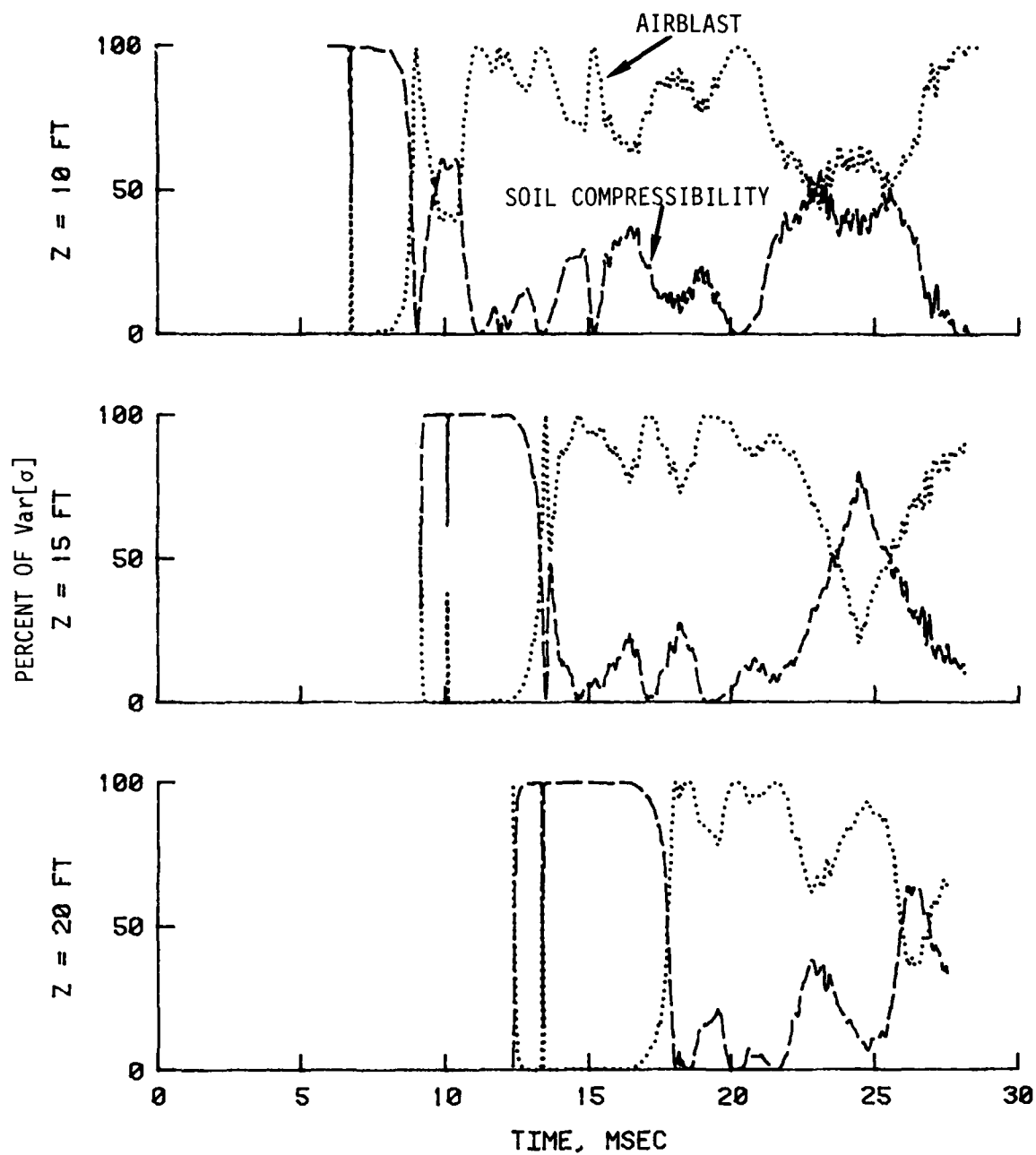


Figure 11. Contribution of input uncertainties to output uncertainty $\text{Var}[\sigma]$

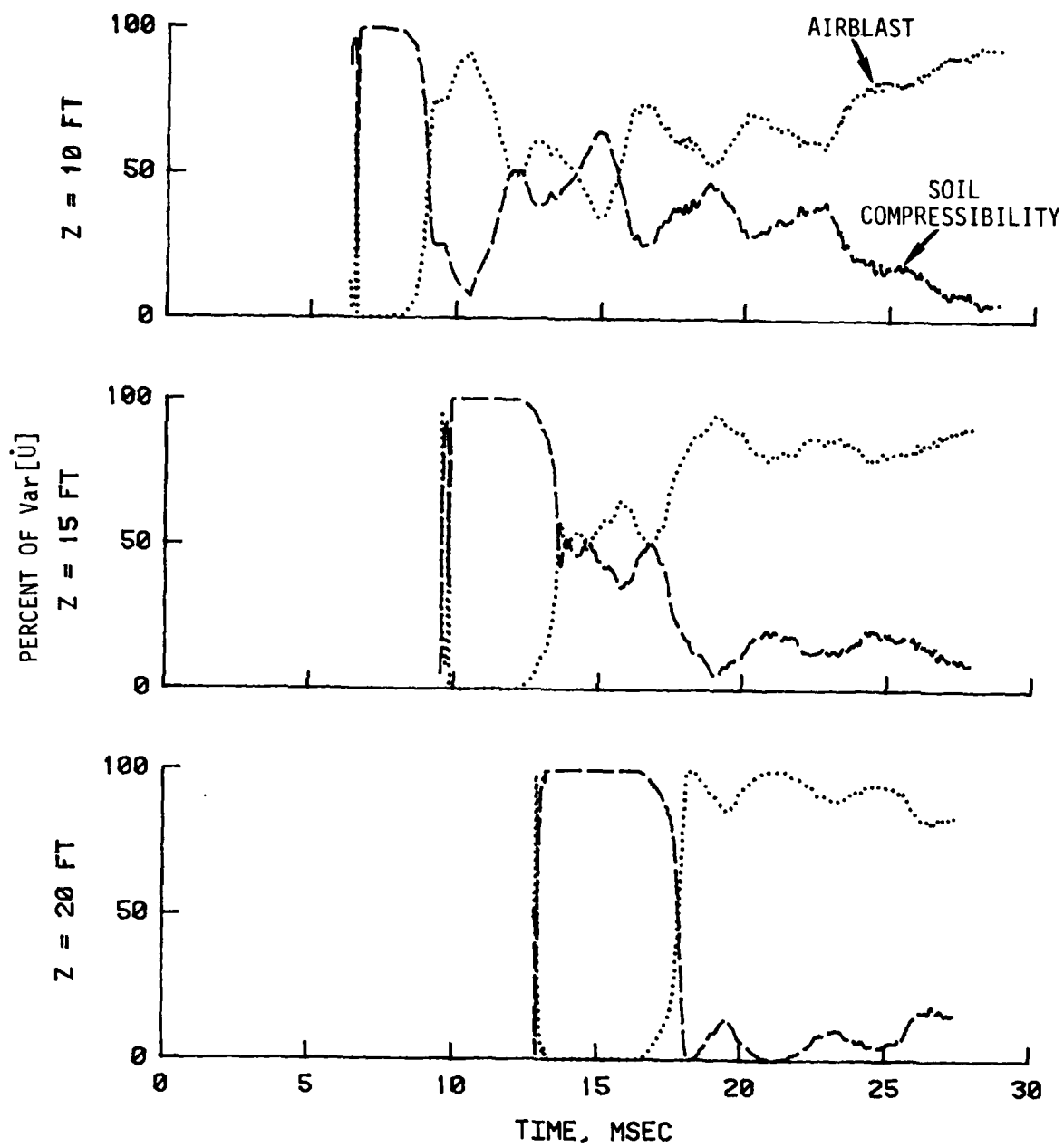


Figure 12. Contribution of input uncertainties to output uncertainty $\text{Var}[U]$

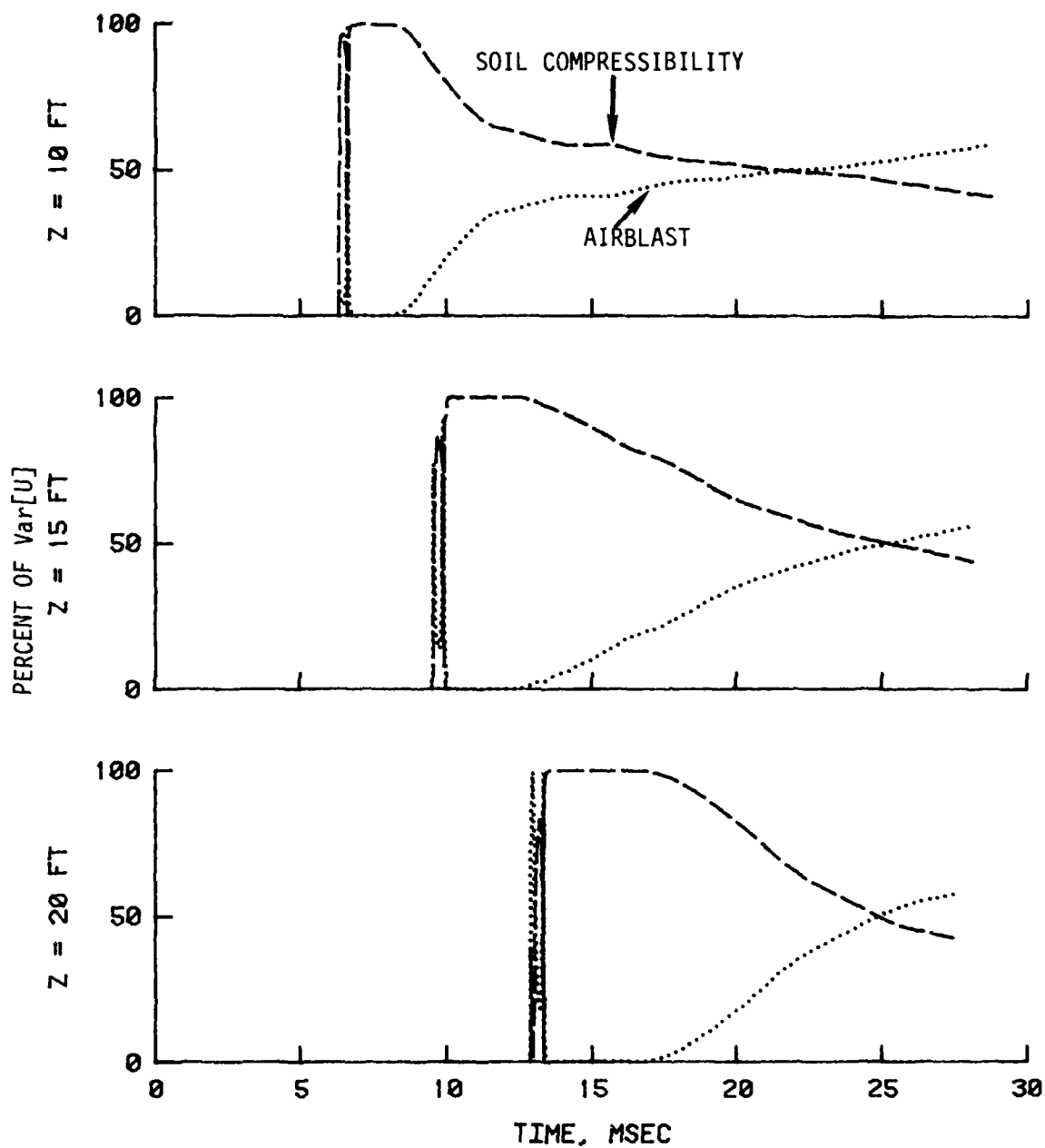


Figure 13. Contribution of input uncertainties to output uncertainty Var[U]

PART V: SUMMARY

18. The partial derivative method has been used to adapt the WES ONED code (a deterministic 1D plane wave propagation code for layered nonlinear hysteretic media) into a probabilistic code referred to as PONE^D. The partial derivatives are evaluated numerically using finite-difference approximations. For a problem containing n input random variables, application of PONE^D would require $2n+1$ deterministic ONED calculations. Within the PONE^D code, computations are made at successive times at selected depths so that the time histories of the expected value and the variance of the dependent variables (stress, particle velocity, and particle displacement) can be constructed. PONE^D also computes and prints out the explicit contributions of each of the input random variables to the overall dispersion of the various output quantities (dependent variables). To demonstrate the application of the solution technique, a probabilistic wave propagation analysis is conducted for an actual explosive test where the stress-strain properties of soil and the applied airblast pressure are treated as random variables. Finally, PONE^D is evaluated against a closed-form probabilistic solution for a two-layered elastic medium where the location of the layer interface is treated as a random variable (Appendix A).

REFERENCES

- Benjamin, J. R. and Cornell, C. A. 1970. Probability, Statistics and Decision for Civil Engineers, McGraw-Hill, New York.
- Haugen, E. B. 1968. Probabilistic Approaches to Design, Wiley, Inc., New York.
- Jackson, J. G., Jr. 1982 (Jul). "Site Characterization for Probabilistic Ground Shock Predictions," Miscellaneous Paper SL-82-8, U. S. Army Engineer Waterways Experiment Station, CE, Vicksburg, Miss.
- Mrakar, P. F. 1978 (Nov). "Application of an Implicit Linear Statistical Analysis to the Estimation of the Resistance of a Reinforced Concrete Beam-Column," Miscellaneous Paper N-78-7, U. S. Army Engineer Waterways Experiment Station, CE, Vicksburg, Miss.
- Radhakrishnan, N. and Rohani, B. 1971 (Nov). "A One-Dimensional Plane Wave Propagation Code for Layered Nonlinear Hysteretic Media," Technical Report S-71-12, U. S. Army Engineer Waterways Experiment Station, CE, Vicksburg, Miss.
- Rohani, B. 1982 (Jun). "Probabilistic Solution for One-Dimensional Plane Wave Propagation in Homogeneous Bilinear Hysteretic Materials," Miscellaneous Paper SL-82-7, U. S. Army Engineer Waterways Experiment Station, CE, Vicksburg, Miss.

Table 1

ONED Calculations Required for Probabilistic Analysis

ONED Calculation	ONED input for a Problem Consisting of m Layers										
	<u>P(t)</u>	<u>SS(1)</u>	<u>T(1)</u>	<u>Y(1)</u>	<u>Z(1)</u>			<u>SS(m)</u>	<u>T(m)</u>	<u>Y(m)</u>	<u>Z(m)</u>
1	μ	μ	μ	μ	μ			μ	μ	μ	μ
2	$\mu+kS$	μ	μ	μ	μ			μ	μ	μ	μ
3	$\mu-kS$	μ	μ	μ	μ			μ	μ	μ	μ
4	μ	$\mu+kS$	μ	μ	μ			μ	μ	μ	μ
5	μ	$\mu-kS$	μ	μ	μ			μ	μ	μ	μ
.
.
.
.
.
.
2(4m+1)	μ	μ	μ	μ	μ			μ	μ	μ	$\mu+kS$
2(4m+1)+1	μ	μ	μ	μ	μ			μ	μ	μ	$\mu-kS$

Note: μ = mean value; S = standard deviation.

APPENDIX A: COMPARISON OF CODE CALCULATION WITH ANALYTICAL SOLUTION

1. In this appendix, the PONE code is evaluated against a closed-form probabilistic solution for a two-layered linear elastic medium subjected to a step pulse at the free surface. Wave propagation conditions and input parameters for this problem are given in Figure A1. In this problem the location of the layer interface is treated as a random variable. All other input parameters are assumed to be deterministic. Therefore, the probabilistic analysis of this problem would require three deterministic calculations using the ONED code. As indicated in Figure A1, the mean μ and $\mu \pm kS$ values for the location of the layer interface are 20 and 20 ± 3 ft, respectively (corresponding to $k = 1$).

2. The three deterministic ONED calculations were conducted using the input parameters shown in Figure A1. The calculations were performed for layer interface locations of 20 (mean value μ), 23 ($\mu + S$), and 17 ($\mu - S$) ft. The results of these calculations were processed with PONE in order to obtain the time histories of the expected values and variances of stress σ and particle velocity \dot{U} at selected depths. The probabilistic results are presented in Figures A2 through A5 for selected depths of 0, 10, 20, and 29 ft. Figures A2 and A4 show the expected values of stress $E[\sigma]$ and particle velocity $E[\dot{U}]$, respectively. The standard deviations of stress S_σ and particle velocity $S_{\dot{U}}$ are shown in Figures A3 and A5, respectively. Figures A2 through A5 also contain the results of the analytical solution for the same problem. These figures indicate that the code results and the analytical solution are essentially identical.

3. Comparison of the analytical and code results is useful in that it provides an opportunity to assess the uncertainties that might be introduced in the solution of a problem due to the solution technique itself. In the case of the ONED code, such uncertainties will usually be present because of the numerical discretization of the problem which introduces spurious oscillations in the code output. Figures A2 through A5 clearly demonstrate the types of uncertainties that might be introduced in the solution of the problem due to the numerical algorithm (solution technique) of the ONED code. For example, consider S_σ at $Z = 29$ ft in Figure A3. The standard deviation should be zero up to a time of approximately 56 msec, as indicated by the

analytical solution. The code solution, however, exhibits a small oscillatory response for S_{σ} prior to this time. The magnitude of such uncertainties depends on many parameters such as integration time step, grid size, and the stress-strain properties of the material. To minimize these types of uncertainties, attempts should be made to reduce the spurious oscillations in the ONED code output by using either artificial viscosity or digital filtering.

4. An important observation can be made based on the results of this problem. It is that in the case of a layered medium with a large mismatch in material properties, such as soil over rock, uncertainties in the location of the layer interface will have a significant effect on the dispersion of stress and particle velocity. This effect is more pronounced on the dispersion of particle velocity.

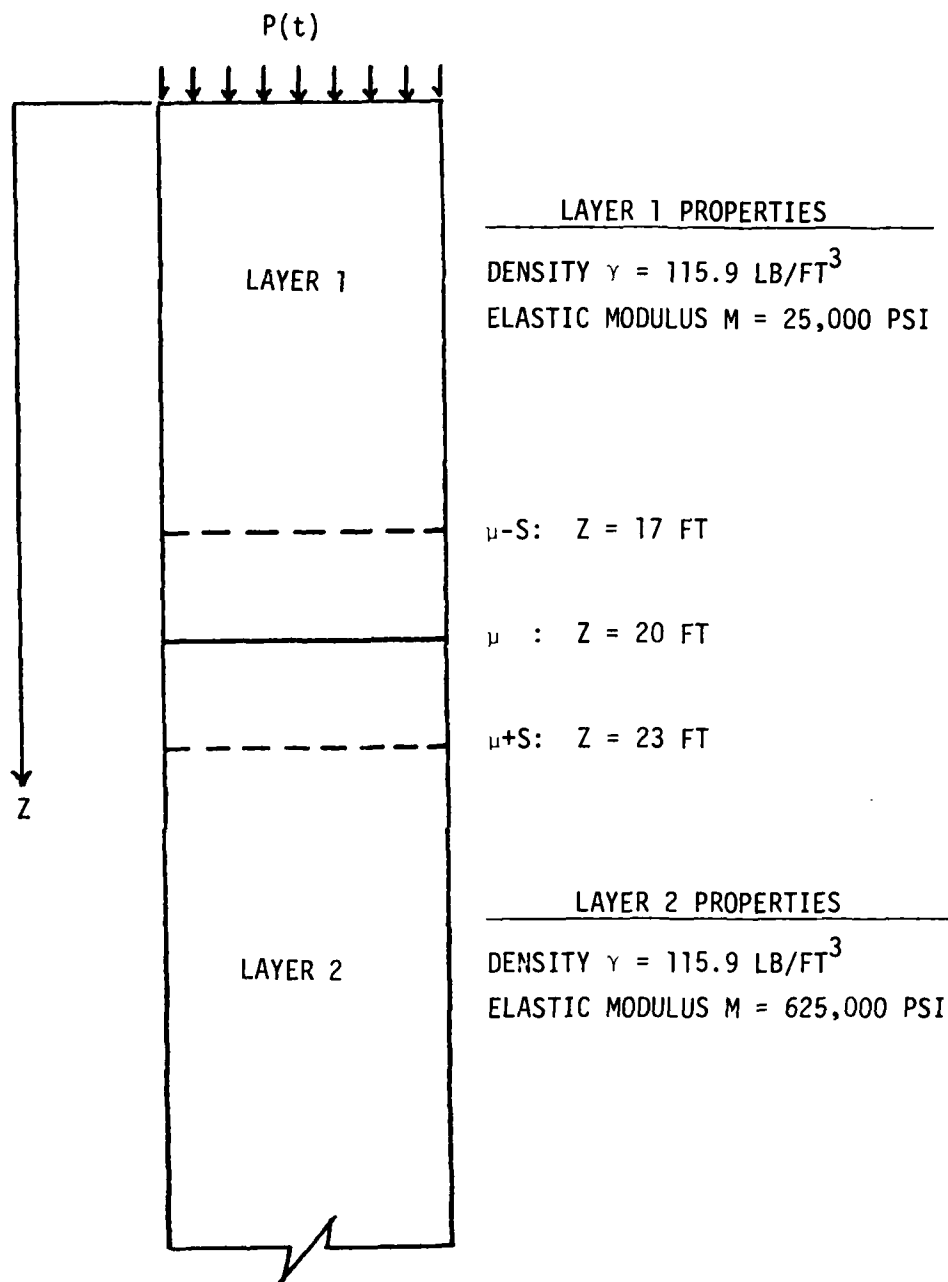


Figure A1. Wave propagation conditions and input parameters

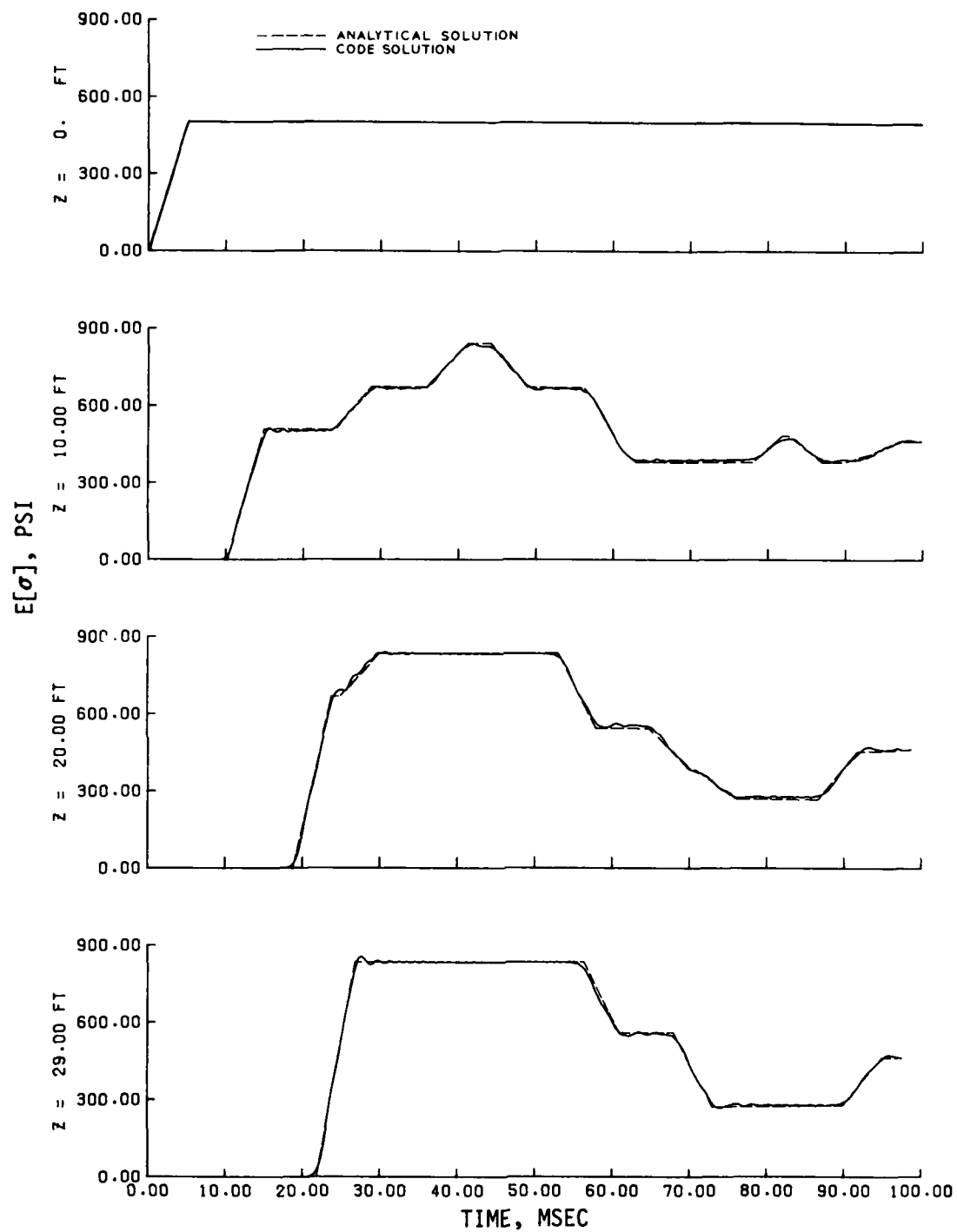


Figure A2. Time history of $E[\sigma]$ at selected depths

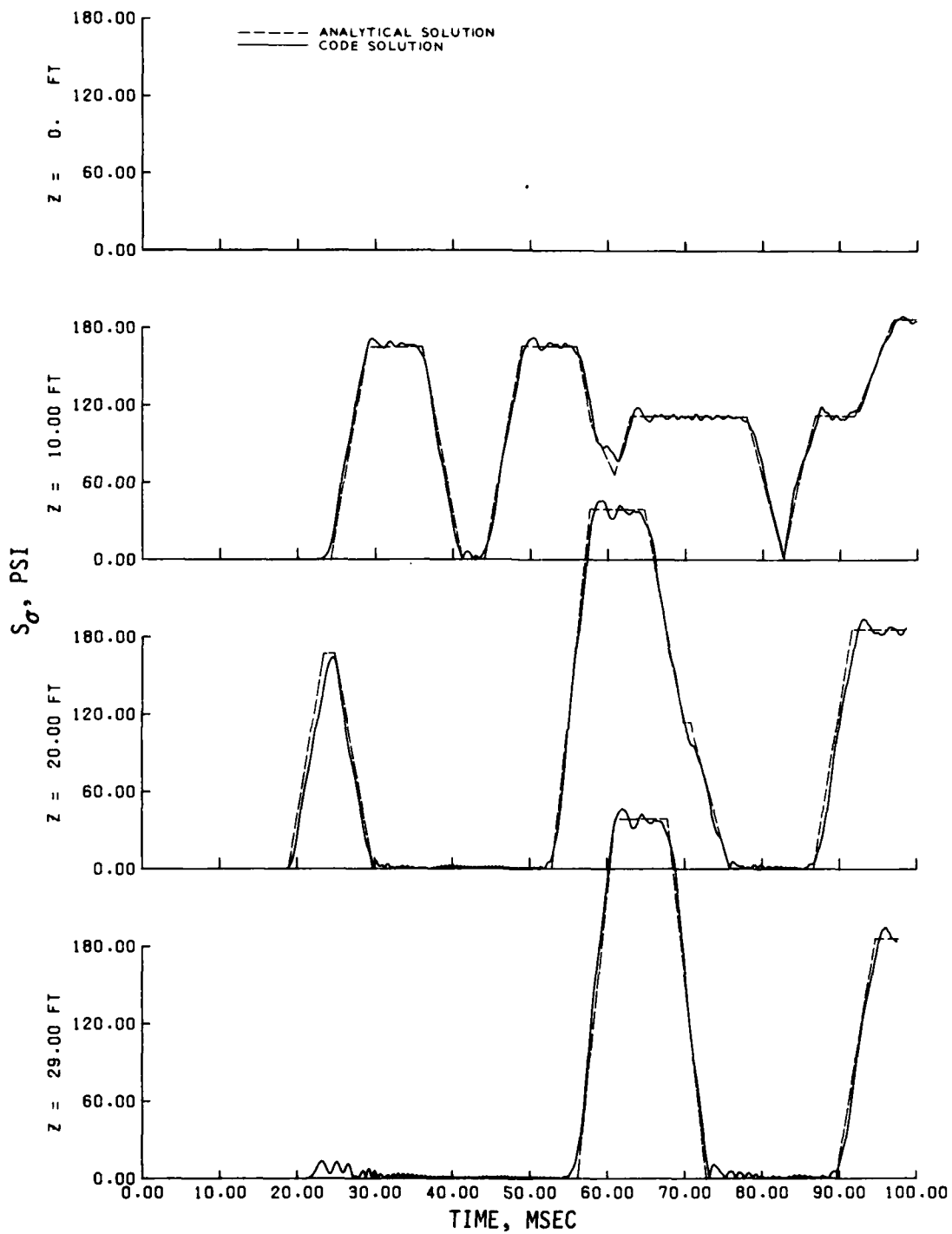


Figure A3. Time history of S_σ at selected depths

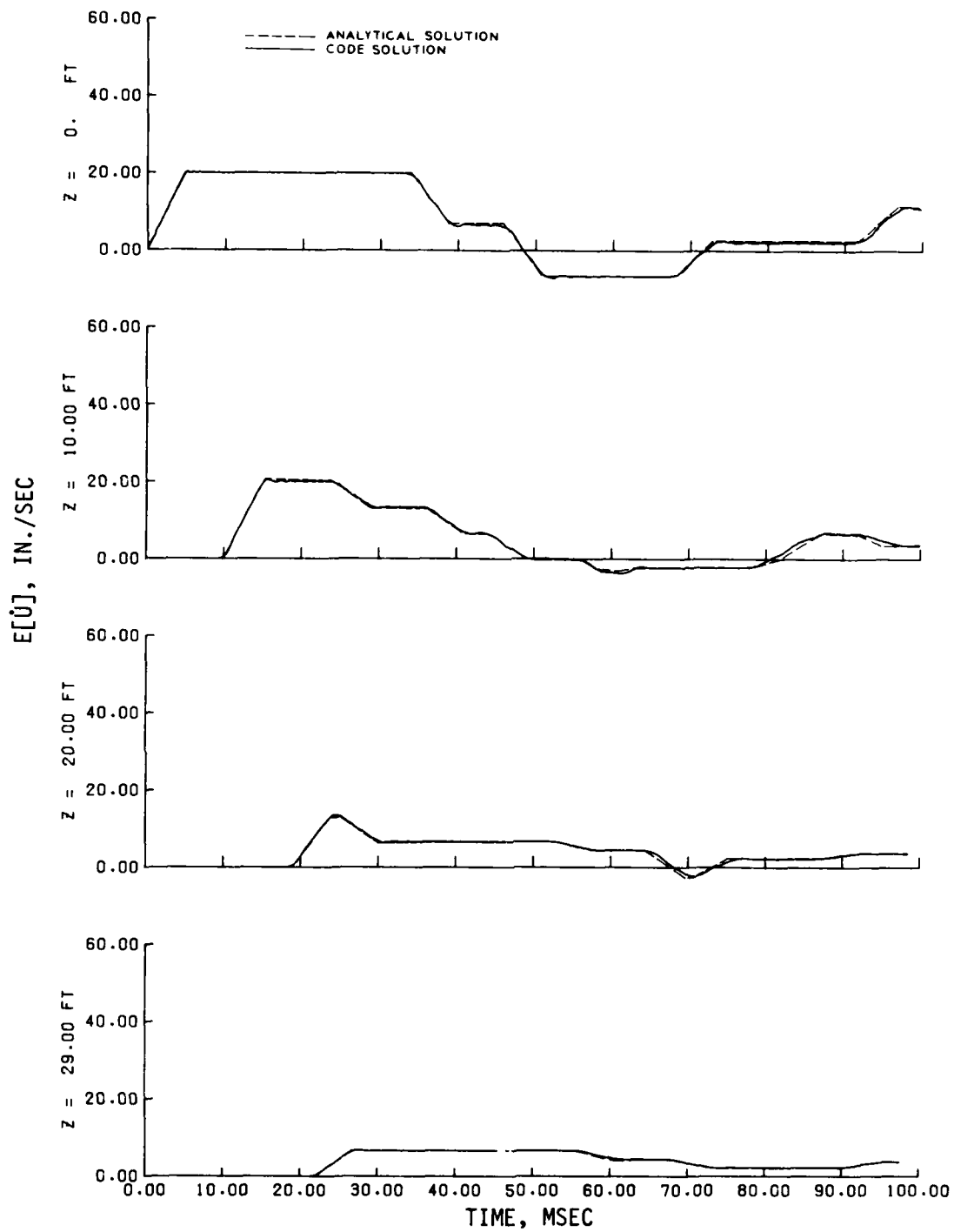


Figure A4. Time history of $E[\dot{U}]$ at selected depths

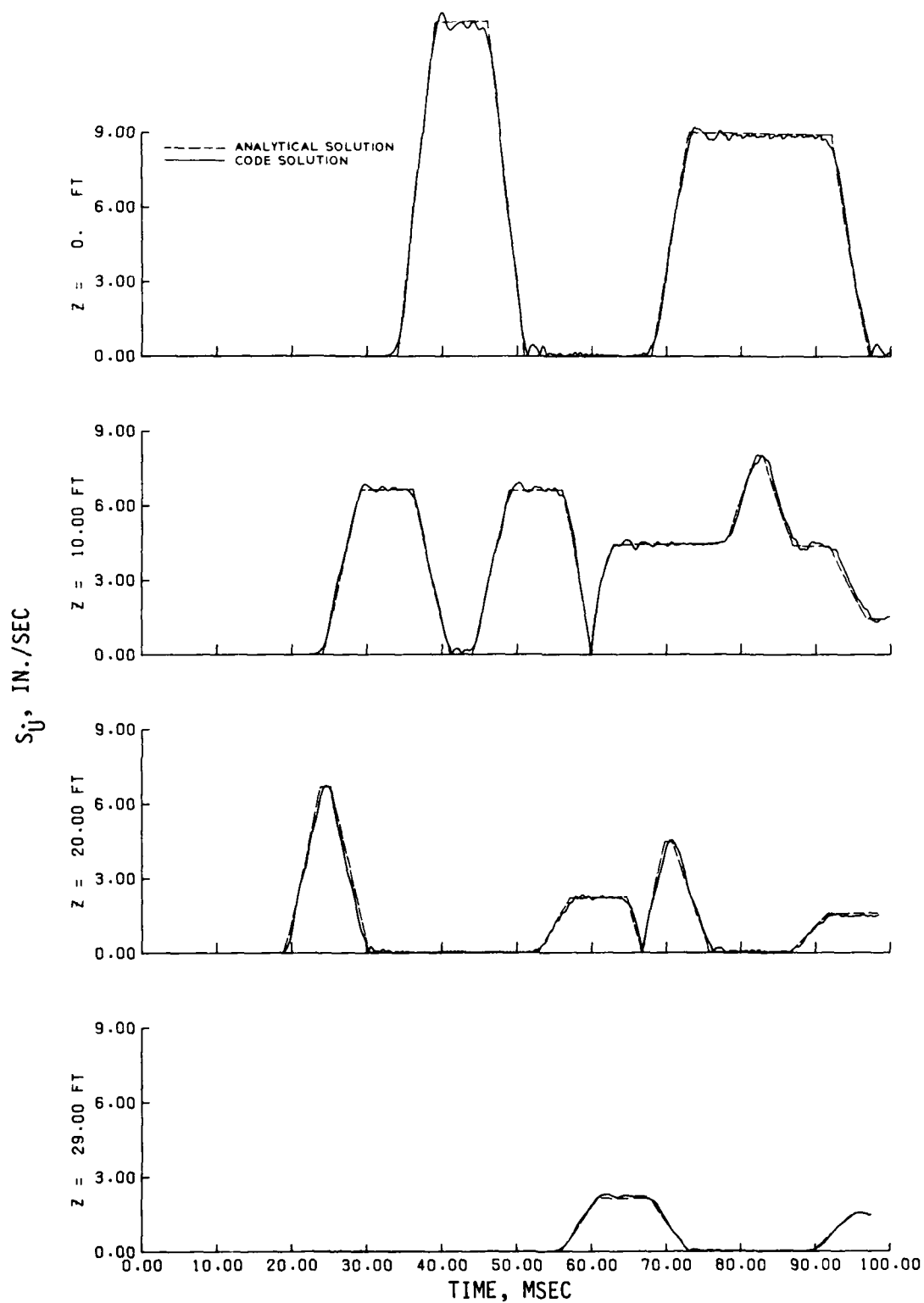


Figure A5. Time history of S_{ij} at selected depths

APPENDIX B

NOTATION

$E[]$	Expectation of a random variable
k	Number of standard deviations above and below mean at which the dependent random variable is evaluated
m	Number of layers in a problem
$P(t)$	Applied surface pressure-time history
$SS(I)$	Stress-strain relation for generic layer I
S_i	Standard deviation of X_i
$T(I)$	Tensile strength for generic layer I
U	Particle displacement
\dot{U}	Particle velocity
$V[]$	Coefficient of variation of a random variable
$Var[]$	Variance of a random variable
X_i	Functionally independent random variable
Y	Functionally dependent random variable
$Z(I)$	Depth to bottom of generic layer I from surface
$\gamma(I)$	Density for generic layer I
μ_i	Mean of X_i
σ	Stress